Molecular Mechanics Studies of Enzyme-Substrate Interactions: The Interaction of L- and D-*N*-Acetyltryptophanamide with α-Chymotrypsin

Georges Wipff,† Andrew Dearing, Paul K. Weiner, Jeffrey M. Blaney, and Peter A. Kollman*

Contribution from the Department of Pharmaceutical Chemistry, School of Pharmacy, University of California, San Francisco, California 94143. *Received September 2, 1981*

Abstract: We have simulated the interaction of α-chymotrypsin with the substrate L-*N*-acetyltryptophanamide (**1**) and the inhibitor D-*N*-acetyltryptophanamide (**2**) as a model for the stereoselective hydrolysis of peptides catalyzed by this enzyme. The noncovalent Michaelis and covalent tetrahedral intermediate complexes of the enzyme active site with each enantiomer were modeled by using molecular mechanics calculations, minimizing the total energy with respect to all geometric degrees of freedom. The lowest energy noncovalent complexes correspond to productive modes of binding that can adopt the geometry of the covalent complexes with some conformational changes; the Michaelis complex for **1** is particularly close to the geometry of the tetrahedral intermediate, while the D complex requires more extensive conformational changes to form the covalent complex. NMR studies have suggested an alternate unproductive mode of noncovalent binding for D-*N*-trifluoroacetyltryptophan with the carbonyl oxygen of the $-NHCOCF_3$ group in the "oxyanion hole". Our calculations suggest that this mode of binding would not be favorable for the analogue D-*N*-trifluoroacetyltryptophan*amide* and predict that this compound should bind to the enzyme in the normal manner. The lowest energy covalent L structure corresponds to the generally accepted model for α-chymotrypsin catalyzed hydrolysis: the α-hydrogen of the substrate points toward the side chain of Met-192, the O of the $CONH_2$ group is in the oxyanion hole, and the NH of the *N*-acetyl group is hydrogen bonded to the C=O of Ser-214. Most of the L-D stereoselectivity is due to the poorer interaction of the $CONH_2$ group of the D enantiomer with the enzyme in the tetrahedral intermediate; the *N*-acetyl group and aromatic side chain also favor the L complex. In particular, the interaction of His-57 with the NH_2 leaving group of the substrate is more favorable in the L complex than the D, which stabilizes the tetrahedral intermediate of **1** relative to **2** and facilitates proton transfer from His-57 to the leaving group. The Michaelis complexes of **1** and **2** with α-chymotrypsin have similar energies, but the tetrahedral intermediate formed by **1** is calculated to be ~9 kcal mol^{-1} more stable than the tetrahedral intermediate formed by **2**, consistent with experimental results that show that the stereoselective recognition of the substrate by α-chymotrypsin occurs in the transition state (modeled by the tetrahedral intermediate) rather than the initial Michaelis complex. This calculated stereoselectivity only occurs when the protein is allowed to be flexible and "relax"; no stereoselectivity is observed when the protein is constrained to the initial X-ray structure. Our results thus provide a structural and energetic model for stereoselective enzyme-substrate interactions.

α-Chymotrypsin (CHT) catalyzes the stereoselective hydrolysis of peptides at L-amino acids.[1,2] Following the kinetic studies that delineated the functional and steric requirements of substrates for catalysis,[3] crystallographic studies have characterized the molecular interactions between the enzyme and the substrate.[4-13]

We have studied the interaction of the substrate L-*N*-acetyltryptophanamide (**1**) and the inhibitor D-*N*-acetyltryptophanamide (**2**) with CHT using molecular mechanics calculations in order

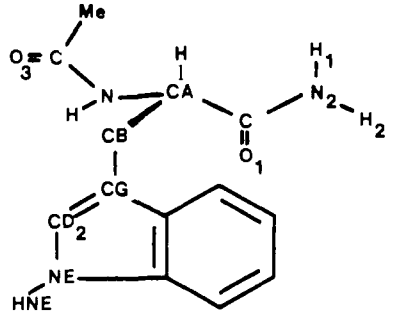

1, 2

to evaluate the ability of molecular mechanics to model enzyme-ligand (E-L) interactions and understand the basis for the stereoselectivity of CHT-catalyzed hydrolysis. We have modeled both the noncovalent Michaelis and covalent tetrahedral intermediate complexes (to represent the transition state) of **1** and **2** with CHT, starting with the X-ray crystal structures of α-chymotrypsin and its tosyl complex:

$$E + L \rightarrow [E\cdots L]_{noncovalent} \rightarrow [E\text{-}L]_{covalent} \rightarrow \ldots \rightarrow \text{products}$$

† Permanent address: Institut de Chimie, BP 296/R8, 67008 Strasbourg, Cedex, France.

Previous investigations into the use of molecular mechanics calculations for modeling enzyme-ligand interactions have been encouraging.[14-24] Platzer et al. studied different conformations

(1) Blow, D. M. In "The Enzymes", 3rd ed.: Adademic Press: New York, 1971; Vol. III, p 185 and 207 and references cited therein.
(2) Hein, G. E.; Niemann, C. *J. Am. Chem. Soc.* **1962**, *84*, 4487 and 4495.
(3) Platt, A.; Niemann, C. *Proc. Natl. Acad. Sci. U.S.A.*, **1963**, *50*, 817. Boter, H. L.; Hooms, A. J. *Biochem. Pharm.* **1967**, *16*, 1563. Bechet, J. J.; Dupaix, A.; Roucoux, C. *Biochemistry* **1973**, *12*, 2566. Gratecos, D.; Guy, O.; Rovery, M.; Desnuelle, P. *Biochem. Biophys. Acta* **1969**, *175*, 82. Bender, M. L. "Mechanisms of Homogeneous Catalysis from Protons to Proteins"; Wiley: New York, 1971; p 108. Cohen, S. G.; Milovanovic, A.; Shultz, R. M.; Weinstein, S. Y. *J. Biol. Chem.* **1969**, *244*, 2664. Cohen, S. G.; Lo, W. L. *Ibid.* **1970**, *245*, 5718. Dupaix, A.; Bechet, J. J.; Roucous, C. *Biochemistry* **1973**, *12*, 2559 Hayashi, Y.; Lawson, W. B. *Ibid.* **1969**, *244*, 4158. Rumsh, L. D.; Volkova, L. I.; Antokov, V. K. *FEBS Lett.* **1970**, *9*, 64.
(4) Blow, D. M. *Isr. J. Chem.* **1974**, *12*, 483.
(5) Steitz, T. A.; Henderson, R.; Blow, D. M. *J. Mol. Biol.* **1969**, *46*, 337.
(6) Bernstein, F. C.; Koetzle, T. F.; Williams, G. J. B.; Meyer E. F., Jr.; Brice, M. D.; Rodgers, J. R.; Kennard, O; Schimanouchi, T.; Tasumi, M. *J. Mol. Biol.* **1977**, *112*, 535.
(7) Birktoft, J. J.; Blow, D. M. *J. Mol. Biol.* **1972**, *68*, 187.
(8) Vandlen, R. L.; Tulinsky, A. *Acta Crystallogr., Sect. B* **1971**, *B27*, 437; **1973**, *B29*, 1309.
(9) Blow, D. M. *Acc. Chem. Res.* **1976**, *9*, 145. Rodgers, P. S.; Goaman, L. C. G.; Blow, D. M. *J. Am. Chem. Soc.* **1976**, *98*, 6690. Blow, D. M.; Steitz, T. A. *Annu. Rev. Biochem.* **1970**, *39*, 63. Fersht, A. R.; Blow, D. M.; Fastrez, J. *Biochemistry* **1973**, *12*, 2035. Blow, D. M.; Birktoft, J. J.; Hartley, B. S. *Nature (London)* **1969**, *221*, 337.
(10) Fersht, A. R.; Sperling, G. J. *J. Mol. Biol.* **1973**, *74*, 137.
(11) Henderson, R. *J. Mol. Biol.* **1970**, *54*, 341. Henderson, R.; Steitz, T. A.; Wright, C. S.; Hess, G. P.; Blow, D. M. *Colo. Spring Harbor Symp. Quant. Biol.* **1971**, *36*, 63 and references cited therein.
(12) Vandlen, R. L.; Tulinsky, A. *Biochemistry* **1973**, *12*, 4193. Tulinsky, A.; Mavridis, I.; Mann, R. F. *J. Biol. Chem.* **1978**, *253*, 1074.
(13) Cohen, G. H.; Silverton, E. W.; Matthews, B. W.; Braxton, H.; Davies, D. R. *J. Mol. Biol.* **1969**, *44*, 129. Davies, D. R.; Cohen, G. H.; Silverton, E. W.; Braxton, H.; Matthews, B. W. *Acta Crystallogr., Sect. A* **1969**, *A25*, 5182. Segal, D. M.; Powers, J. C.; Cohen, G. H.; Davies, D. R.; Wilcox, P. E. *Biochemistry* **1971**, *10*, 3728.

0002-7863/83/1505-0997$01.50/0

of L-amino acids within the active site of CHT (with a rigid model of the active site) and found a correlation between the calculated and the experimental relative free energies of binding.[14] De Tar, using a different force field, has compared the stabilization of the tetrahedral intermediates derived from L- and D-amino acids,[15,16] calculating the corresponding "steric energies", which, corrected by an electrostatic factor, accounted for the stereoselectivity in hydrolysis of L- and D-*N*-acetyltryptophanamide and L- and D-*N*-acetylphenylalanineamide. However, a more complete model of enzyme–ligand interactions requires the evaluation of the structure and energy of *both* the covalent enzyme–substrate complex and the initial noncovalent Michaelis complex; this is the purpose of our study.

The dissociation constant for **1** ($K_s \approx K_M = 5.3 \times 10^3$) is similar to the inhibition constant for **2** ($K_i = 2.7 \times 10^{-3}$).[25] However, the L–D rate difference for the hydrolysis of **1** and **2** is $\sim 10^5$, which corresponds to a difference in the free energies of activation of ~ 7 kcal mol^{-1}.[25] Therefore, the high L–D stereoselectivity of CHT is not due to the initial noncovalent enzyme–substrate (Michaelis) complexes but rather to differential stabilization of the corresponding transition states, since K_M for the L substrate and K_i for the D inhibitor are nearly identical.[26–29]

Acylation of the enzyme is rate limiting for amide hydrolysis.[30,31] Nucleophilic attack by the hydroxyl oxygen of Ser-195 of CHT on the carbonyl carbon of the substrate and proton transfer from the hydroxyl group of Ser-195 to His-57 lead to the formation of the tetrahedral intermediate:

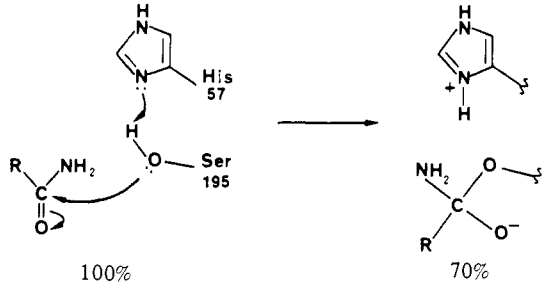

The tetrahedral intermediate decomposes to yield the acyl enzyme by proton transfer from the imidazolium of His-57 to the amino leaving group of the substrate. We use the tetrahedral intermediates of **1** and **2** with CHT to represent the transition state (the transition state is probably close to the tetrahedral intermediate), assuming that the enzyme–ligand interactions for **1** and **2** differ in the transition state by an amount comparable to that of the corresponding tetrahedral intermediates. The transition state for the CHT-catalyzed hydrolysis of amides appears to correspond to the acylation step of the reaction,[30,31] but whether it involves the formation rather than the decomposition of the tetrahedral intermediate formed during acylation is not clear.[32–34] Our calculations are more relevant for the formation rather than the decomposition of the tetrahedral intermediate.

Methods

Starting geometries were taken from the X-ray crystal structures of uncomplexed CHT[8] (2.8-Å resolution) for the noncovalent complexes and tosyl–CHT[6,7] (2.0-Å resolution) for the tetrahedral intermediates. Since it is computationally impractical to include all the atoms of the enzyme in the calculation, we have selected only those atoms that are likely to interact significantly with the substrate. All residues within 7 Å of any atom of the tosyl inhibitor have been included in the model of the active site of CHT (41–43, 55–59, 102, 142, 143, 189–196, 213–222, 225–228); the side chains of residues extending away from the substrate (Phe-41 and Trp-215) were replaced by hydrogen, giving a total of 266 atoms for the active-site model. The uncomplexed CHT structure was first energy refined with a restraint of 10 kcal mol^{-1} Å^2 ($E_{restraint} = \sum_{atoms} 10D^2$, where D is the distance between the current and initial Cartesian coordinates of each atom) on all atoms to remove several initial bad contacts, the root-mean-square difference between the initial and (partially) relaxed structure was 0.17 Å.

Nucleophilic attack by Ser-195 on the substrate results in transfer of the Ser-195 hydroxyl proton to His-57, while Asp-102 remains negatively charged.[35,36] Therefore, our model includes a neutral His-57 for the noncovalent complex and a protonated His-57 for the tetrahedral intermediate. However, considerable evidence suggests that the pK_a of His-57 is between 6.5 and 7.0, so that His-57 is $\sim 50\%$ protonated at physiological pH.[37,38] In order to assess the role of the charge of His-57 on the noncovalent binding of **1** and **2**, we also evaluated noncovalent complexes with a protonated His-57.

Models for the interaction of **1** and **2** with CHT were built on an Evans and Sutherland color picture system 2 with the program CHEM.[39] This program allows the user to change the location of different molecules relative to each other, adjust torsional angles, and monitor interatomic distances while displaying the molecules in color and stereo. This type of interactive refinement proved to be essential in finding the lowest energy structures.

The active site of CHT has been described in terms of four interaction sites located tetrahedrally around the α-carbon of the substrate that bind the aromatic side chain, the acylamide group, the α-hydrogen, and the $-CONH_2$ group of the substrate.[40,41] We did not try to satisfy these "rules" a priori, fixing only the O_i amido oxygen of the substrate in the oxyanion hole (defined by the NH groups of Gly-193 and Ser-195), and the indole ring in the "hydrophobic pocket" of CHT. Several different starting conformations were evaluated for the noncovalent and covalent protein–ligand complexes to scan as much conformational space as possible. We designate the noncovalent Michaelis complexes by LM and DM, and the covalent tetrahedral intermediates by LT and DT.

For the noncovalent Michaelis complexes, three D and eleven L structures were built and optimized. Several different "hydrolyzable" structures were evaluated, starting with substrate conformations that could lead to a tetrahedral intermediate and adjusting the conformation and position of the substrate in the active site, keeping the amido oxygen near the oxyanion hole and the indole ring in the hydrophobic pocket. In each of these models, the Ser-195 OH group points away from His-57 (as in the X-ray structure of uncomplexed CHT), so that the proton transfer to the histidine that must eventually occur will require a rotation of the side chain of Ser-195 toward His-57. To determine if such a

(14) Platzer, K. E. B.; Momamy, F. A.; Scheraga, H. A. *Int. J. Pept. Protein Res.* **1972**, 201.
(15) De Tar, D. F. *J. Am. Chem. Soc.* **1981**, *103*, 107.
(16) De Tar, D. F., *Biochemistry* **1981**, *20*, 1730.
(17) Gelin, B. R.; Karplus, M. *Biochemistry* **1979**, *18*, 1256.
(18) Mc Cammon, J. A.; Karplus, M. *Proc. Natl. Acad. Sci. U.S.A.* **1979**, *76*, 3585.
(19) Pincus, H. R.; Burgess, A. W.; Scheraga, H. A. *Biopolymers* **1976**, *15*, 2485.
(20) Levitt, M. *J. Mol. Biol.* **1974**, *82*, 393.
(21) Warshel, A.; Levitt, M. *J. Mol. Biol.* **1976**, *103*, 227.
(22) Hagler, A. T.; Lifson, S.; Dauber, P. *J. Am. Chem. Soc.* **1979**, *101*, 5122; *Ibid.* **1979**, *101*, 5131 and references cited therein.
(23) Lesk, A. M.; Chothia, C. *J. Mol. Biol.* **1980**, *136*, 225.
(24) Honig, B.; Ray, A.; Levinthal, C. *Proc. Natl. Acad. Sci. U.S.A.* **1976**, *73*, 1974.
(25) Huang, H. T.; Niemann, C. *J. Am. Chem. Soc.* **1951**, *73*, 1541; *Ibid.* **1962**, *84*, 4495.
(26) Knowles, J. R. In "Peptides"; North-Holland: Amsterdam, 1968; p 310.
(27) Kraut, J. *Annu. Rev. Biochem.* **1977**, *46*, 331 and references cited therein.
(28) Johnson, C. H.; Knowles, J. R. *Biochem. J.* **1966**, *101*, 56.
(29) Applewhite, T. H.; Niemann, C. *J. Am. Chem. Soc.* **1959**, *81*, 2208.
(30) Cunningham, L. W. *Compr. Biochem.* **1965**, *16*, 85 and references cited therein.
(31) Bender, M. L.; Killheffer, J. V. *CRC Crit. Rev. Biochem.* **1973**, 149.
(32) Fink, A. L. *Acc. Chem. Res.* **1977**, *10*, 233.
(33) Lucas, E. C.; Caplow, M. *J. Am. Chem. Soc.* **1972**, *94*, 960. Bender, M. L.; Philip, M. *Ibid.* **1973**, *95*, 1665. Ferhst, A.; Requena, Y. *Ibid.* **1971**, *93*, 7079. Frankfater, A.; Kezdy, F. J. *Ibid.* **1971**, *93*, 4039. Hunkapiller, M. W.; Forgac, M. D.; Richards, J. H. *Biochemistry* **1976**, *15*, 5581.
(34) Caplow, M. *J. Am. Chem. Soc.* **1969**, *91*, 3639.
(35) Markley, J.; Ibanez, I. *Biochemistry* **1976**, *15*, 3399.
(36) Kollman, P. A.; Hayes, D. M. *J. Am. Chem. Soc.* **1981**, *103*, 2955.
(37) Hess, G. P.; McCoon, J.; Ku, E.; McConkey, G. *Philos. Trans. R. Soc. London, Ser. B* **1970**, *257*, 80.
(38) Bender, M. L.; Clement, G. E.; Kezdy, F. J.; d'A Meck, H. *J. Am. Chem. Soc.* **1964**, *86*, 3680.
(39) CHEM, a program for molecular modeling, written by A. Dearing (unpublished).
(40) Hein, G.; Nieman, C. *Proc. Natl. Acad. Sci. U.S.A.* **1961**, *47*, 1311; *J. Am. Chem. Soc.* **1962**, *84*, 4495.
(41) Cohen, S. G.; Milanovic, A.; Schultz, R. M.; Weinstein, S. Y. *J. Biol. Chem.* **1969**, *244*, 2664. Cohen, S. G. and Schultz, R. M., *J. Biol. Chem.* 1968, *243*, 2607.

rotation could modify the relative energies of the L and D noncovalent complexes, we reoptimized each of the lowest energy L and D (LM1, DM1) models following rotation of the Ser-195 side chain, resulting in structures LM1r and DM1r, respectively. We also modeled noncovalent complexes (LM3–LM11, DM3) that should be unable to hydrolyze (usually because of lack of stabilization of the developing oxyanion) for comparison with the hydrolyzable complexes. Several different nonproductive binding modes were considered. The NH_2 leaving group can be oriented away from solvent such that rotation of the $CONH_2$ group to place the amino portion in solvent would cause a loss of the oxyanion hole stabilization for the O_1 carbonyl oxygen. An "inverse" binding mode is also possible (suggested by NMR results[42]), where the carbonyl oxygen of the *N*-acetyl group rather than the O_1 of the $CONH_2$ group lies in the oxyanion hole. The four lowest energy noncovalent conformations reported by Platzer et al.[14] (A, B, C, H) were also used as starting points for energy minimization (LM8–LM11). Although these nonhydrolyzable complexes lack the critical interactions near the oxyanion hole, they can form other favorable hydrogen bonds, which might stabilize these structures relative to the productive hydrolyzable modes of binding.

For the covalent complexes, two different models for **1** and **2** were built. LT1 corresponds to the generally accepted model for the tetrahedral intermediate: the α-hydrogen points toward the side chain of Met-192 and the *N*-acetyl group points toward the solvent, with its NH group hydrogen bonded to the carbonyl oxygen of Ser-214. The indole-ring NH group interacts with the carbonyl oxygen of Ser-217. LT2 differs in that the *N*-acetyl points inside the hydrophobic pocket toward Val-213 and the indole NH points toward the –OH group of Tyr-228. For the D enantiomer, DT1 has its α-hydrogen directed toward Val-213 and the *N*-acetyl group toward the top of the hydrophobic pocket with its carbonyl oxygen toward the NH of Gly-216, while DT2 has its α-hydrogen near Ser-214 and the *N*-acetyl group toward solvent.

Energy calculations were performed with the molecular mechanics software package AMBER[43] on a VAX-11/780, by using a force field similar to that of Gelin and Karplus,[17] differing mainly in our explicit inclusion of potential hydrogen-bonding interactions. CH, CH_2, and CH_3 groups are treated as united atoms. The energy of the system is represented in terms of bond stretching, bending, torsional, and nonbonded (van der Waals and electrostatic) energies:

$$E_{\text{total}} = \sum_{\text{bonds}} K_r(r - r_{\text{eq}})^2 + \sum_{\text{angles}} K_\vartheta(\vartheta - \vartheta_{\text{eq}})^2 + \sum_{\text{dihedrals}} \frac{K}{2}(1 + \cos(n\phi - \gamma)) + \sum_{i<j} \frac{B_{ij}}{R_{ij}^{12}} - \frac{A_{ij}}{R_{ij}^{6}} + \frac{q_i q_j}{\epsilon R_{ij}}$$

All atoms were allowed to move during energy refinement, using analytical gradients with conjugate gradient minimization until the root-mean-square energy gradient was less than 0.1 kcal $Å^{-1}$. Although this convergence criterion is insufficient to guarantee a true local minimum, comparison with calculations (on the covalent complexes LT1 and DT1) in which the refinement was continued to a root-mean-square energy gradient of 0.02 kcal $Å^{-1}$ showed that the structures and relative energies did not change significantly (during the additional ~500 iterations, the absolute energies of LT1 and DT1 decreased by only 0.5 kcal mol^{-1} and 0.7 kcal mol^{-1}, respectively, and the root-mean-square shift for each was 0.1 Å).

The partial atomic charges in all residues used in evaluating the electrostatic energy come from ab initio calculations on related models.[44] These charges and most of the force field parameters are given in ref 45 (the partial atomic charges for the "reactive end" of the substrate are included as supplementary material for this paper). Electrostatic energies are evaluated by using a dielectric constant of $\epsilon = R_{ij}$ (the distance between nonbonded atoms *i* and *j*) in order to reduce the interactions between relatively distant charged residues. Warshel has shown that the effective dielectric constant for short-range ionic interactions in water is smaller than the bulk dielectric and increases (roughly linearly) with the ionic separation.[46] The preliminary study of Rees on the internal effective dielectric constant of cytochrome *c* also suggests that the dielectric constant within proteins increases with charge separation.[47] By weighting short-range electrostatic interactions more strongly than long range, one finds that use of a distance-dependent dielectric constant indirectly allows for polarization and charge-transfer contributions to the contact ion-pair interaction (as opposed to the solvent-separated ion-pair).

Initial calculations on the covalent L and D complexes were performed to evaluate the effect of restraints on the calculated energies. These trial runs showed that the enzyme active site must be able to "relax" in order to differentiate the two enantiomers; with the entire active site restrained, the L and D complexes have the same total energy. The L complex becomes progressively more stable than the D as the restraints on the active site are released: by ~3 kcal mol^{-1} when all the α-carbons are restrained, by ~9 kcal mol^{-1} when only the α-carbons at the terminus of each peptide are restrained, and by ~12 kcal mol^{-1} when all atoms are allowed to relax. Therefore, optimization of each complex was performed in two stages. In stage one each atom of the active site and substrate was restrained to its initial position with a weight of 10 kcal mol^{-1} $Å^{-2}$ in order to relieve initial bad contacts without allowing the large energy gradients of these atoms to cause artificial movement elsewhere. Convergence for this first stage was achieved after about 80 iterations, with root-mean-square difference between the initial and refined structure of ~0.1 Å. In stage two the entire system was allowed to energy refine while retaining restraints only on the motion of the α-carbons at the terminus of each peptide in the active-site model. This approach provides a reasonable representation of small sections of proteins without explicit inclusion of the entire protein molecule, while still allowing limited motion of the active-site region. Convergence required about 1000 iterations for this second stage.

Our original calculations on the covalent L and D complexes led to hydrogen bonds in the oxyanion hole that were unreasonably short (1.23–1.30 Å). Although neglect of a repulsive H···O van der Waals term is satisfactory for neutral hydrogen bonds, the ionic hydrogen bonds present in the oxyanion hole of the tetrahedral intermediate require an explicit H···O van der Waals repulsion to compensate for the unusually strong electrostatic H···O attraction. Therefore, subsequent calculations on the covalent complexes included an explicit 10–12 hydrogen-bond potential.[17,48] This led to hydrogen-bond lengths of 1.6–1.7 Å but otherwise essentially the same structures and relative energies as obtained in the original calculations.

The major factors responsible for the calculated L–D stereoselectivity have been analyzed by dissecting the total energy for each complex into component energies, i.e., the active site energy, the substrate energy, and the active site–substrate interaction energy. The active site–substrate interaction energy is further broken down into the interaction energy of the substrate with each of the seven separate peptides of the active site and also into the interaction of the entire active site with each of the four functional groups (the hydrogen, *N*-acetyl, aromatic side chain, and the $-CONH_2$) of the substrate.

Results

1. Noncovalent Michaelis Complexes. The structural characteristics and conformations of the energy-refined noncovalent complexes are summarized in Table I. Table II lists the energies for all the noncovalent complexes for **1** and **2**, and the enzyme–substrate energies for the lowest energy structures are broken down into component interaction energies in Table III. Table IV (supplementary material) contains the breakdown of the total energy into intra- and intermolecular components. LM1r (Figure 1), which is similar to the most stable tetrahedral intermediate LT1, is the lowest energy noncovalent complex. The most stable noncovalent complex for the D enantiomer, DM1r (Figure 2), is calculated to be 0.3 kcal mol^{-1} higher in energy than LM1r. These structures resulted from rotation of the side chain of Ser-195 toward His-57 in the best "native conformation" (as in the original x-ray structure) structures LM1 and DM1. As the side chain of Ser-195 rotates toward His-57 in the LM1 and DM1 models (forming LM1r and DM1r, respectively), the L–D energy difference decreases from 2.3 to 0.3 kcal mol^{-1}. The energy of the substrate and active site increase during this process for the L enantiomer but remains essentially constant for the D enantiomer. Rotation of Ser-195 also results in an enhanced enzyme–substrate interaction energy for the L enantiomer.

The only parts of the active site whose interaction with **1** and **2** make differences of more than 1 kcal/mol are groups 5 (containing Met-192 and the oxyanion hole) and 6 (containing Ser-214). For the productive binding modes (LM1, LM1r, LM2,

(42) Bosshard, H. R. *Isr. J. Chem.* **1974**, *12*, 495.
(43) Weiner, P.; Kollman, P. *J. Comput. Chem.* **1981**, *2*, 287.
(44) See Lehn and Wipff (Lehn, J. M.; Wipff, G. *J. Am. Chem. Soc.* **1980**, *102*, 1347) for tetrahedral intermediate and Hayes and Kollman (Hayes, D. M; Kollman, P. A. *Ibid.* **1976**, *98*, 3335) for the amino acid residues.
(45) Blaney, J. M.; Weiner, P. K.; Dearing, A.; Kollman, P. A.; Jorgensen, E. C.; Oatley, S.; Burridge, J. M.; Blake, C. C. F. *J. Am. Chem. Soc.* **1982**, *104*, 6424.
(46) Warshel, A. *J. Phys. Chem.* **1979**, *83*, 1640.
(47) Rees, D. *J. Mol. Biol.* **1980**, *141*, 323.
(48) We used a 10–12 potential with R_0 = 1.8 Å and a $E_{\min}$ = –0.5 kcal mol^{-1}. This attraction is, of course, in addition to the predominant electrostatic attraction in these H-bond interactions.

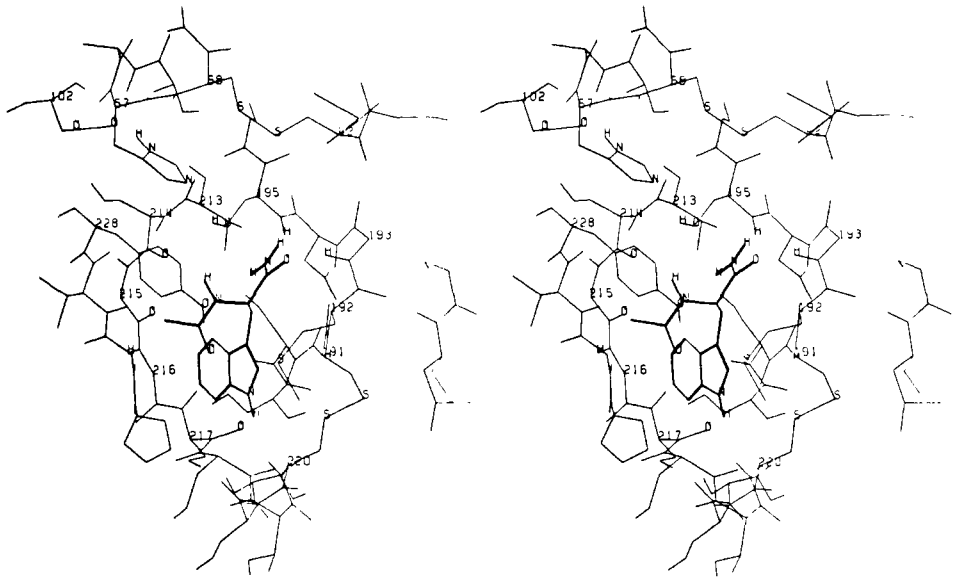

Figure 1. Energy-refined noncovalent complex for 1 (LM1r). Labeled residues include His-57, Cys-58, Asp-102, Cys-191, Met-192, Gly-193, Ser-195, Val-213, Ser-214, Trp-215, Gly-216, Ser-217, and Tyr-228. Heteroatoms and hydrogen-bonding hydrogens are labeled for the substrate.

Table I. Structural Characteristics of the Refined Covalent and Noncovalent CHT-AcTRN Complexes

	torsional angles[a]							direction of[d]		
complex	ϕ	X_1	X_2	ψ	β	d_1[b]	d_2[c]	$C_\alpha H$	Ac	C=O_1
LT1	234	298	159	61	−1	1.62	1.69	Met-192	solvent	O^- hole
LT2	216	311	288	102	24	1.61	1.81	Met-192	Val-213	O^- hole
DT1	110	49	57	53	181	1.64	1.66	Val-213	Ser-214	O^- hole
DT2	138	57	123	314	1	1.64	1.83	Ser-214	solvent	O^- hole
DM1	146	53	97	244	1	3.14	4.15	Gly-215	solvent	O^- hole
DM2	131	42	103	310	4	1.91	1.79	Gly-215	solvent	O^- hole
DM3	101	56	160	293	3	4.97	6.34	Cys-191	O^- hole	solvent
LM1	223	285	130	57	356	1.96	1.76	Met-192	solvent	O^- hole
LM2	225	319	169	134	3	2.71	1.67	Gly-215	Val-213	O^- hole
LM3	219	200	32	53	177	7.23	7.40	Ser-214	Ser-195	Ser-217
LM4	271	306	343	305	0	1.84	1.97	Cyx-191	Cyx-220	O^- hole
LM5	237	305	131	315	186	2.33	4.13	Met-192	Gly-216, Ser-214	outside the O^- hole
LM6	248	42	277	77	181	6.01	4.18	O^- hole, solvent	solvent	His-57
LM7	250	55	219	339	0	1.99	1.84	Met-192	solvent	O^- hole
LM8	256	178	58	63	353	6.97	7.35	Ser-214, Gly-216	His-57, Ser-214	Gly-216, Ser-217
LM9	264	306	334	310	354	1.72	1.97	Met-192	Ser-214	O^- hole
LM10	251	46	280	182	179	6.51	5.68	O^- hole	solvent	Gly-216
LM11	230	48	274	102	1	6.41	4.65	O^- hole	solvent, Met-192	Gly-215

[a] ϕ = C-C_A-N-C(acetyl), X_1 = N-C_A-C_B-C_G, X_2 = C_A-C_B-C_G-C_{D_2}, ψ = N_2-C-C_A-N, β = C_A-N-C-O_3. The atom labels are defined in the drawing of 1 and 2. [b] d_1 = $O_1\cdots$HN of Gly-193. [c] d_2 = $O_1\cdots$HN of Ser-195. [d] Characterizes roughly toward which part of the active site C_AH, Ac, and C=O_1 point. However, in several cases, it is hard to define precisely the orientation of the substrate. A stereoscopic view of the structures and the Cartesian coordinates of these structures can be obtained from the authors.

Table II. Total Energies of Noncovalent Complexes

hydrolyzable complexes	total energy, kcal mol^{-1}	nonhydrolyzable complexes	total energy, kcal mol^{-1}
LM1	−48.5	DM3	−40.2
LM2	−36.7	LM3	−46.2
DM1	−46.2	LM4	−43.4
DM2	−43.3	LM5	−44.3
LM1r	−50.1	LM6	−42.1
DM1r	−49.8	LM7	−38.3
$LM1^+$	−67.1	LM8	−28.9
$LM2^+$	−66.3	LM9	−31.9
$DM1^+$	−69.9	LM10	−40.1
		LM11	−47.1
		DM_3^+	−63.5

DM1, DM1r, DM2), the best interaction with groups 5 and 6 is with the *least* stable LM2 structure, caused by the tighter contacts of LM2 with the active site, resulting in more favorable van der Waals interactions with the substrate and group 6. This is compensated by increased strain in the enzyme and substrate, so that the LM2 complex is overall less stable than the other noncovalent complexes. The substrate in the DM1 complex interacts less favorably with group 5 (the oxyanion hole); this is the only complex where O_1 of the $CONH_2$ group is outside of the oxyanion hole, toward solvent. The *N*-acetyl group forms only weak interactions with the active site in the noncovalent complexes. For LM1, the contacts $CH_3CONH\cdots O{=}C$ Ser-214 (2.36 Å) and indole-NH···O=C Ser-217 (2.50 Å) are too long to form strong hydrogen bonds. Table II shows that protonation of His-57 favors the noncovalent complex for **2** over **1** by 2.8 kcal mol^{-1}. This is not due to any single dominant interaction but rather to the sum of several small interactions.

None of the "nonhydrolyzable" models produced complexes that were more stable than the productive mode of binding found for LM1 and DM1 (Table II), although most of them have an enzyme–substrate interaction energy similar to that found for LM1 (a complete breakdown of the component interaction energies is available from the authors on request). The best interaction energy is in LM4, with O_1 in the oxyanion hole, $-NH_2$ hydrogen bonded to Ser-214 (rather than in solvent), the acetyl oxygen O_3 hydrogen

Table III. "Hydrolyzable" Noncovalent Complexes: Interaction Energy Analysis[a]

		all substrate with groups 1–7 of the active site							all active site with groups 1–4 of AcTRN			
complex	group	1	2	3	4	5	6	7	$C_\alpha H$	NHAc	site Ch	$OCNH_2$
LM1	VdW	−0.3	−0.8	−0.0	−0.3	−26.7	−23.3	−5.8	−3.0	−7.8	−37.3	−9.2
	el	−0.1	−0.1	−0.3	−0.0	−2.0	−1.8	−0.1	−1.1	−1.5	0.6	−2.3
	tot	−0.5	−0.9	−0.4	−0.3	−28.7	−25.1	−5.7	−4.1	−9.3	−36.7	−11.5
LM2	VdW	−0.2	−1.2	−0.1	−0.2	−25.1	−27.7	−6.6	−2.9	−13.5	−36.2	−8.5
	el	−0.1	−0.0	0.0	−0.0	−4.5	−1.9	0.2	−2.3	−1.5	−0.2	−2.0
	tot	−0.3	−1.2	−0.0	−0.3	−29.6	−29.6	−6.4	−5.2	−15.1	−36.4	−10.5
DM1	VdW	−0.4	−1.9	−0.1	−0.3	−23.7	−22.8	−5.4	0.8	−9.9	−38.3	−7.0
	el	−0.1	−0.2	−0.0	0.0	−0.6	−5.6	0.0	−3.7	−0.9	0.1	−1.1
	tot	−0.4	−0.2	−0.1	−0.3	−24.3	−28.3	−5.4	−2.9	−10.8	−38.4	−8.9
DM2	VdW	−0.3	−0.6	−0.0	−0.3	−25.6	−23.2	−6.3	−2.3	−8.4	−36.8	−8.7
	el	−0.1	0.0	0.2	0.0	−2.4	−4.1	0.0	−0.7	−3.9	0.4	−2.3
	tot	−0.4	−0.6	0.1	−0.3	−28.0	−27.3	−6.3	−3.0	−12.3	−36.4	−11.0
LM1r	VdW	−0.4	−0.9	−0.0	−0.3	−28.1	−24.5	−5.6	−2.8	−9.3	−38.4	−9.3
	el	−0.2	−0.1	−0.4	−0.0	−2.8	−2.4	0.1	−1.7	−1.8	0.6	−2.8
	tot	−0.6	−1.0	−0.4	−0.2	−30.9	−26.9	−5.5	−4.5	−11.1	−37.8	−12.1
DM1r	VdW	−0.3	−2.1	−0.1	−0.2	−21.5	−23.1	−7.5	−0.4	−8.7	−39.3	−6.3
	el	−0.0	−0.1	0.0	0.0	−1.3	−4.7	−0.1	−3.3	−1.7	−0.4	−0.8
	tot	−0.4	−2.1	−0.1	−0.2	−22.8	−27.8	−7.6	−3.7	−10.4	−39.7	−7.1
$LM1^+$	VdW	−0.3	−0.8	−0.0	−0.3	−26.1	−23.1	−5.9	−2.4	−8.0	−37.0	−9.0
	el	−0.1	0.8	−0.3	0.0	−2.2	−0.8	0.1	0.1	0.0	0.7	−3.3
	tot	−0.5	0.0	−0.3	−0.3	−28.3	−23.9	−5.8	−2.5	−8.0	−36.3	−12.3
$DM1^+$	VdW	−0.4	−2.4	−0.1	−0.3	−23.0	−22.9	−5.6	−2.0	−7.0	−38.4	−7.3
	el	−0.1	0.4	0.0	0.0	−0.5	−5.6	0.0	0.5	−4.3	6.2	−2.2
	tot	−0.5	−2.1	−0.1	−0.3	−23.5	−28.5	−5.6	−1.5	−11.3	−32.2	−9.5
$LM2^+$	VdW	−0.2	−1.1	−0.1	−0.2	−24.9	−28.3	−7.3	−2.9	−13.6	−36.7	−8.9
	el	−0.1	−0.2	0.1	−0.0	−4.1	−2.2	−0.6	−0.3	−3.8	−0.6	−2.5
	tot	−0.3	−1.3	0.0	−0.3	−29.0	−30.5	−7.9	−3.2	−17.4	−37.3	−11.4

[a] See footnote of Table VI.

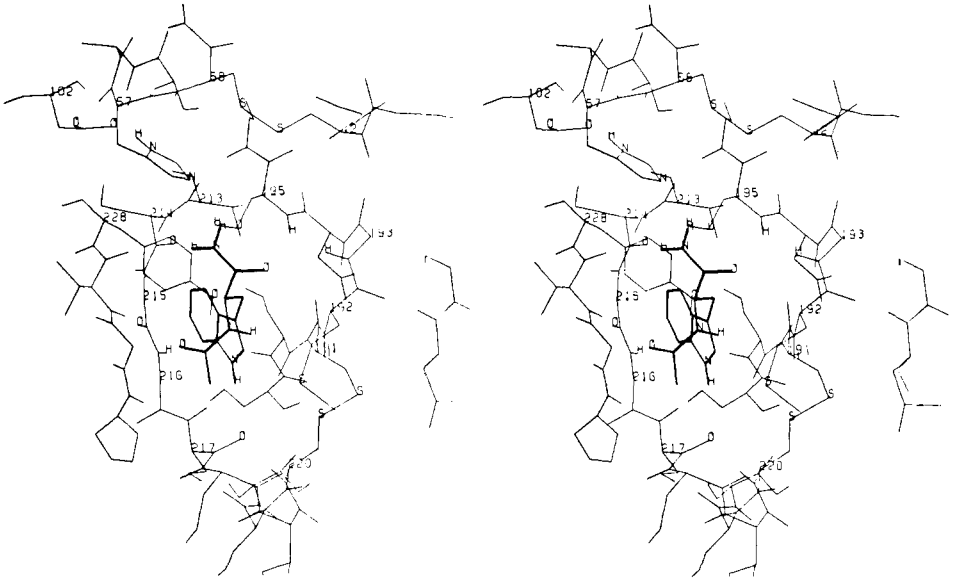

Figure 2. Energy-refined noncovalent complex for **2** (DM1r).

bonded to the NH of Met-192, and the indole ring forming favorable van der Waals interactions deep in the hydrophobic pocket. The "inverse" binding mode for **1** (where the binding sites for the *N*-acetyl and $CONH_2$ groups are switched, placing the acetyl oxygen O_3 in the oxyanion hole instead of the amido oxygen O_1) led to a structure (LM3) that was only 2 kcal, mol^{-1} higher in energy than LM1, suggesting that this mode of binding is possible for the L enantiomer. The *N*-acetyl group of the substrate in LM3 and the $CONH_2$ group from LM1 interact similarly with the oxyanion hole, while the $CONH_2$ of LM3 interacts better with Ser-214–Ser-217 than does the *N*-acetyl of LM1. The enzyme–substrate interaction energy is more favorable with the inverse binding mode, but this is offset by a higher internal energy for the substrate and active site. The D inverse binding mode (DM3, Figure 3) was calculated to be ~6 kcal mol^{-1} higher in energy than the normal mode of binding (DM1). The poorest interaction energy is in LM8, with the *N*-acetyl group of the substrate between His-57 and Ser-214, the NH of the *N*-acetyl pointing toward solvent (without favorable contacts), and the $CONH_2$ group toward Gly-216 such that this structure receives no stabilization by the oxyanion hole. We also repeated the calculations on the nonhydrolyzable complexes with a protonated His-57, obtaining qualitatively the same results as with a neutral histidine.

2. Covalent (Tetrahedral Intermediate) Complexes. The structural characteristics and conformations of the energy-refined covalent complexes are summarized in Table I. Table V lists the

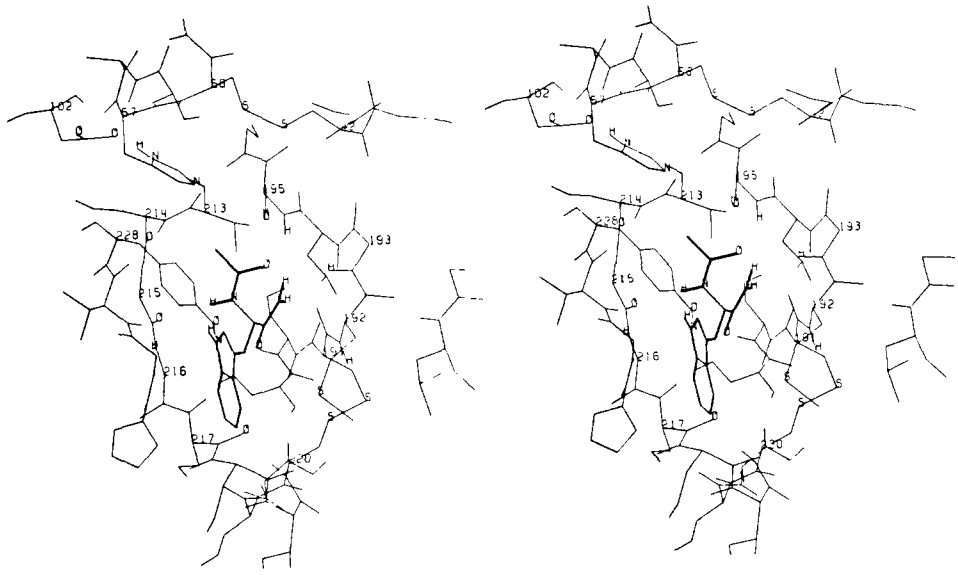

Figure 3. Energy-refined noncovalent complex for **2** corresponding to an "inverse" binding mode (DM3).

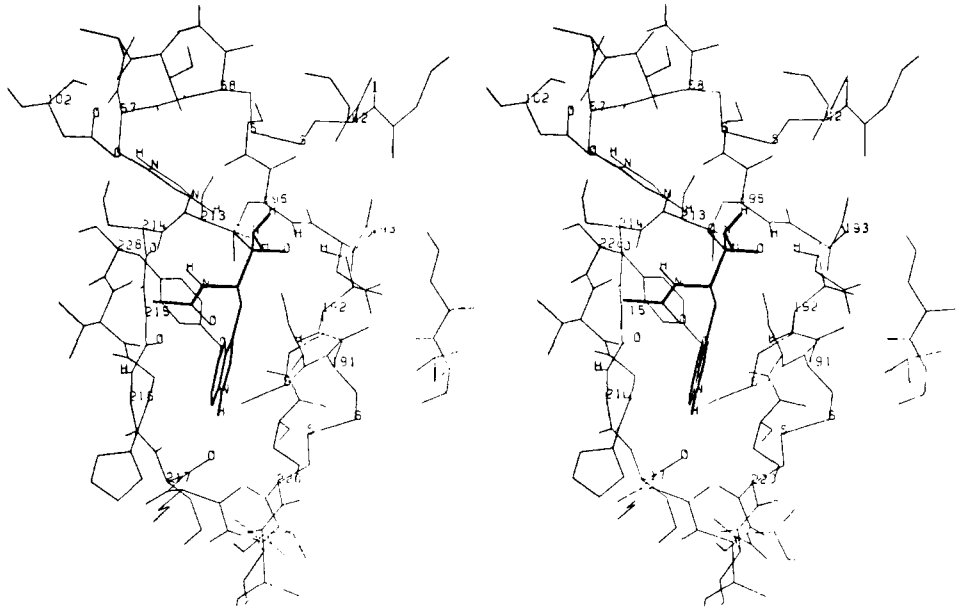

Figure 4. Energy-refined covalent complex for **1** (LT1).

energies for the four covalent complexes for **1** and **2**. The most stable tetrahedral intermediate (LT1, Figure 4) is ~17 kcal mol^{-1} more stable than the alternate L structure (LT2) and 9.3 kcal mol^{-1} more stable than the best D structure (DT1, Figure 5). The alternate model for the tetrahedral intermediate of **2** (DT2) is ~3 kcal mol^{-1} higher in energy than DT1. LT1 is favored by both the total energy and the enzyme–substrate interaction energy, primarily in the electrostatic terms.

The more favorable enzyme–substrate interaction energy in the LT1 complex is the main contributor to the calculated L–D stereoselectivity. Table VI shows that the interaction of the substrate with the critical groups 2 (containing His-57), 5 (containing Met-192 and the oxyanion hole), and 6 (containing Ser-214) varies greatly between the four covalent complexes (LT1, LT2, DT1, DT2).

The amido nitrogen of the $-CONH_2$ group of the substrate interacts with the His-57 H_{N_ϵ} proton most favorably in the LT1 structure (N–H distance = 1.77, 1.95, 2.30, and 2.88 Å in LT1, DT2, LT2, and DT1, respectively). For group 5, the strongest interaction is between the O_1^- of the substrate and the oxyanion hole, even though the O_1^- is in the oxyanion hole in all four covalent complexes. A further division of the energetic contributions of the C–O$^-$ and NH_2 groups with the oxyanion hole shows that the main difference comes from the NH_2 group (−13.5, −8.4, −6.5, −10.6 kcal mol^{-1} in LT1, LT2, DT1, and DT2, respectively) rather than from the C–O$^-$ group (−20.6, −20.2, −19.3, −19.2 kcal mol^1, respectively).

The interaction of each residue in group 6 with the substrate was analyzed. Ser-214 interacts better with the substrate in LT1 (−4.2 kcal mol^{-1}) than in LT2, DT1, or DT2 (−2.0–1.0, and −1.6 kcal/mol^{-1}, respectively); the energy difference is mainly electrostatic, due to the *N*-acetyl NH···O=C Ser-214 hydrogen bond (1.83 Å) in LT1. LT1 and DT1 are stabilized relative to LT2 and DT2 by the substrate indole-NH···O=C Ser-217 hydrogen bond, which is reflected by the Ser-217–indole ring-interaction energies (−5.5, −2.5, −5.1, and −1.3 kcal mol^{-1} for LT1, LT2, DT1, and DT2, respectively).

Comparison of the interaction of the four groups of the substrate with the active site (Table VI) shows that the largest contribution to the calculated stereoselectivity comes from the interaction of His-57 with the NH_2 of the H_2N–C–O$^-$ group (primarily electrostatic), consistent with the observation that the leaving amino group is closest to His-57 in the most stable tetrahedral intermediate, LT1. The α-hydrogen of the substrate interacts weakly

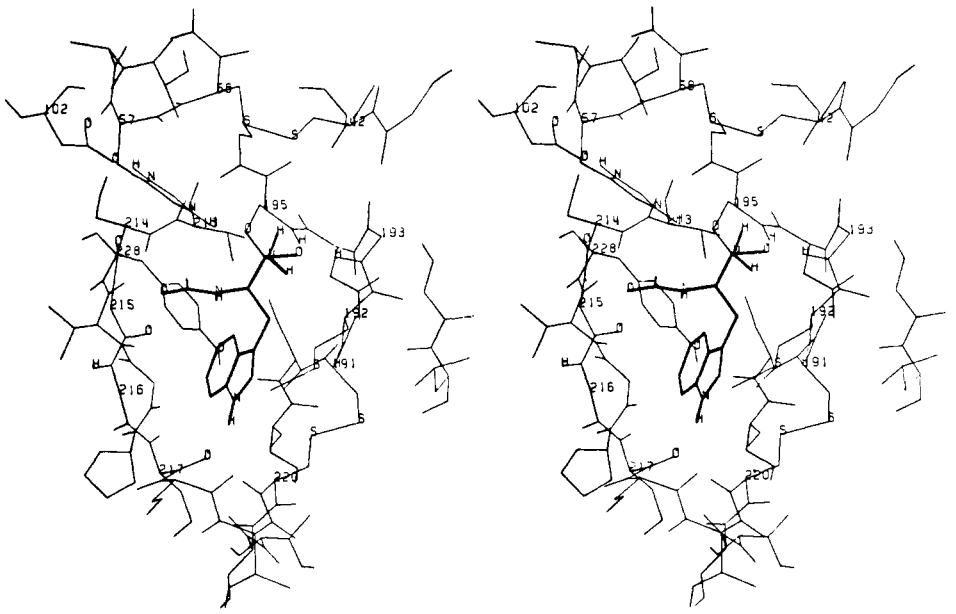

Figure 5. Energy-refined covalent complex for **2** (DT1).

Table V. Covalent Complexes; Total Energies and Substrate–Enzyme Energies

complex		total energy[a]	energy components[b] E_{as}	E_{sub}	INT	Cst
LT1	int	86.9	80.5	6.4		
	VdW	−175.1	−131.9	8.1	−51.3	
	el + HB	−25.3	19.4	−6.1	−38.6	
	E_T	−110.9 (−99.2)[c]	−32.0	8.4	−89.9	2.6
LT2	int	100.9	88.5	12.4		
	VdW	−172.5	−124.8	7.0	−54.7	
	el + HB	−24.6	12.2	−4.4	−32.4	
	E_T	−93.4 (83.1)[c]	−24.1	15.0	−87.1	2.8
DT1	int	94.6	84.7	9.9		
	VdW	−179.0	−136.7	7.1	49.4	
	el + HB	−19.8	16.4	−8.3	−27.9	
	E_T	−101.6 (−89.0)[c]	35.6	8.7	−77.3	2.6
DT2	int	88.4	81.3	7.2		
	VdW	−168.6	−127.8	8.0	−48.9	
	el + HB	−21.1	15.0	−8.2	−27.9	
	E_T	−98.9 (88.9)[c]	−31.5	7.0	−76.8	2.4

[a] int is the internal energy (bond stretching + angle bending + torsional energies), VdW is the Van der Waals energy, El + HB is the electrostatic and hydrogen-bond energy. E_T = int + VdW + el + HB + Cst. [b] E_{as} is the energy of the active site (including O_γ of Ser-195), E_{sub} is the energy of the substrate, and INT is the interaction energy between the two. Cst is the energy associated with the constraints. $E_T = E_{as} + E_{sub}$ + INT + Cst. [c] Total energies without the explicit 10-12 hydrogen-bond function.

with the enzyme and does not differentiate the four complexes considered here. The active-site interaction with the *N*-acetyl group is not the best for LT1, although it has the best electrostatic energy due to the *N*-acetyl NH···O=C Ser-214 hydrogen bond. The interaction energy of the *N*-acetyl group with the enzyme is similar in DT1 due to compensating van der Waals interactions. The aromatic side chain interacts with the active site most favorably in LT1, primarily due to more favorable van der Waals contacts (the indole ring is more deeply buried in the hydrophobic pocket).

Discussion

The L–D stereoselectivity of the chymotrypsin-catalyzed hydrolysis of **1** and **2** is not related to the initial noncovalent enzyme–substrate binding (Michaelis complex) but rather to a differential stabilization of the corresponding transition states. The enzyme positions the enantiomers differently with respect to the residues involved in catalysis and, in this fashion, lowers the energy of formation of the transition state for the L enantiomer. Results for the noncovalent complexes show that in addition to the lack of clear L–D differentiation at this stage of the enzymatic reaction, rotation of the Ser-195 side chain may induce relative "strain" in the active site and substrate in the L complex but not the D, thus "setting up" the L enantiomer for hydrolysis. Although the overall energies of the most stable Michaelis complexes (LM1r, DM1r) are nearly identical, the internal energy of the active site and substrate is 4.3 kcal mol^{-1} higher in the LM1r complex, which is compensated by a 4.6 kcal mol^{-1} stronger interaction energy.

The relatively weak interactions found between the *N*-acetyl group of the substrate and the enzyme in the LM1 and DM1 structures is consistent with experimental results that demonstrate that the *N*-acetyl group is important in stabilizing the transition state but has little effect on the initial noncovalent complex.[4,27] The *N*-acetyl NH···O=C Ser-214 hydrogen bond does not form in the Michaelis complex, despite the mobility of the substrate, in agreement with experimental results: K_M values for similar substrates are practically independent of the presence or absence in the substrate of hydrogen-bond-donating NH bonds, whereas a hydrogen-bonding interaction is crucial for stereospecificity and for a high rate of hydrolysis. Substitution of the CH_3CONH group by CH_3CONCH_3 would be expected to destabilize the transition state and tetrahedral intermediate but not the Michaelis complex, as shown by experimental results with the closely related substrates *N*-acetyltyrosine and *N*-acetyl-*N*-methyltyrosine.[49] For the D inverse mode of binding (where the binding sites for the *N*-acetyl and $-CONH_2$ groups are switched), the CH_3 of the *N*-acetyl group of **2** is near His-57, consistent with the downfield shift of the CF_3 resonance in the ^{19}F NMR spectrum of *N*-trifluoroacetyl-D-tryptophan upon binding to CHT.[42] However, this structure is less stable than the normal binding mode (DM1) by 6 kcal mol^{-1} and would be expected to be highly unfavorable for the binding of **2**, hence a similar ^{19}F NMR study on the binding of *N*-trifluoroacetyl-D-tryptophan*amide* to CHT should result in only a negligible change in chemical shift (as observed for *N*-trifluoroacetyl-L-tryptophan), indicating a normal mode of binding. Substitution of the $CONH_2$ group of **2** by $-COO^-$ should lead to increased stabilization of DM3 vs. DM1, since in DM3 the interaction of the NH_2 group with the oxyanion hole is repulsive but the interaction with a carboxylate group will be attractive. Also, the substitution of $CONH_2$ by $-COO^-$ will destabilize DM1 due to the loss of the hydrogen bonds from the NH_2 group to H_{N_ϵ}

(49) Caplow, M.; Harper, C. *J. Am. Chem. Soc.* **1972**, *94*, 6508.

Table VI. Covalent Complexes; Interaction Energy Analysis

complex	group	all substrate with groups 1-7 of the active site[a]							all active site with groups 1-4 of AcTRN			
		1	2	3	4	5	6	7	$C_\alpha H$	NHAc	side chain	$^-OCNH_2$
LT1	VdW	−0.9	−3.5	−0.1	−0.3	−19.9	−20.9	−5.9	−2.7	−7.8	−36.4	−4.4
	el + HB	0.5	−14.7	2.3	−0.3	−22.4	−4.1	0.1	2.1	−8.8	1.7	−29.7
	tot[b]	−0.4	−18.0	2.2	−0.6	−42.3	−25.0	−5.8	−0.6	−16.6	38.1	−34.1
LT2	VdW	−0.5	−2.5	−0.1	−0.5	−27.3	−18.2	−5.6	−2.6	−12.3	−34.8	−5.0
	el + HB	0.9	−10.4	2.2	−0.2	−22.8	0.5	−2.6	1.5	−8.0	−2.4	−23.5
	tot	0.4	−12.9	2.1	−0.7	−50.1	−17.7	−8.2	−1.1	−20.3	−37.2	−28.5
DT1	VdW	−0.7	−4.7	−0.2	−0.4	−20.3	−18.0	−5.1	−2.3	−10.4	−32.1	−4.6
	el + HB	0.7	−8.1	2.5	−0.2	−21.2	−1.6	0.0	1.8	−6.6	−2.0	−21.1
	tot	0.0	−12.8	2.3	−0.6	−41.5	−19.6	−5.1	−0.5	−17.0	−34.1	−25.7
DT2	VdW	−0.7	−1.5	−0.1	−0.3	−22.2	−16.6	−7.5	−2.4	−6.9	−35.7	−3.9
	el + HB	0.7	−14.5	3.2	−0.3	−16.6	−0.3	−0.1	2.3	−4.6	0.3	−25.9
	tot	0.0	−16.0	3.1	−0.6	−38.8	−16.9	−7.6	−0.1	−11.5	−35.4	−29.8

[a] Group 1, Phe-41 to Gly-43; group 2, Ala-55 to Gly-59 (contains His-57); group 3, Asn-102; group 4, Gly-142, Leu-143; group 5, Ser-189 to Gly-196 (contains Met-192 and the O^- hole); group 6, Val-213 to Thr-222 (contains Ser-214, Ser-217); group 7, Pro-225 to Tyr-228. [b] VdW and el + HB are the van der Waals and electrostatic plus hydrogen bond group-group interactions energies, respectively. tot = VdW + el + HB. The total interaction energy between AcTRN and the active site (INT) is the sum of the contribution of the different groups.

of His-57 and the carbonyl oxygen of Gly-215. Presumably, this is why the inverse mode of binding is preferred for the anionic *N*-trifluoroacetyl-D-tryptophan over the normal mode of binding.

His-57 is ~50% protonated at physiological pH;[37,38] results obtained with a protonated His-57 in the noncovalent complexes show that the D complex is 2.8 kcal mol^{-1} more stable than the L, suggesting that the initial binding step to CHT may actually favor the D enantiomer slightly. In fact, the K_M for **1** is about double the K_I for **2**, consistent with the general observation that D enantiomers bind ~0.4 kcal mol^{-1} better than L enantiomers to CHT.[50] Thus, it is clear that the high L–D stereoselectivity of CHT is not related to the initial noncovalent enzyme–substrate binding.

Both the energetic and structural results obtained for the tetrahedral intermediates strongly favor the L complex. The interaction most important in differentiating L from D appears to be the hydrogen bonding of the H_{N_ϵ} of His-57 to the NH_2 of the $-CONH_2$ group of the substrate. This interaction stabilizes the tetrahedral intermediate for the L enantiomer and also facilitates the protonation of the NH_2 leaving group in the most stable complex (LT1). LT1 and DT2 are the only complexes where the nitrogen lone pair of the substrate leaving amino group points directly toward H_{N_ϵ} of His-57; in LT2 and DT1 it points toward Ser-195. For the lowest energy D complex (DT1), the His-57 H_{N_ϵ} proton is closer to the Ser-195 O_γ than the amino leaving group of the substrate, suggesting that reprotonation of the O_γ to regenerate the starting Michaelis complex is more likely to occur than protonation of the leaving group.

An *N*-acetyl NH···O=C Ser-214 hydrogen bond also appears to be important in determining L–D stereoselectivity, since the lowest energy tetrahedral intermediate (LT1) has the best interaction with Ser-214. Experimental comparison of the closely isosteric analogues, *N*-acetyl-L- and *N*-acetyl-phenylalanine and *O*-acetyl-L- *O*-acetyl-D β-phenyllactate shows that replacement of the amido NH of the *N*-acetyl group by an oxygen atom greatly reduces the stereoselectivity of deacylation of the acyl–enzyme intermediate, consistent with a critical hydrogen-bonding role for this group.[51] This interaction was also proposed by De Tar[16] as contributing ~1.8 kcal mol^{-1} to the L–D stereoselectivity. The importance of the oxyanion hole stabilization has been pointed out in both the covalent and noncovalent complexes, although it appears that this stabilization is not essential for L–D discrimination.

The results emphasize the role of small active-site conformational changes in stereoselectivity, since calculations with a completely rigid active site show no stereoselectivity. Finally, the noncovalent L complex appears to be structurally predisposed toward forming the tetrahedral intermediate, as the LM1r and LT1 conformations are very similar, while the D complex will require substantial conformational change to form a tetrahedral intermediate. Thus, conversion of LM1r to LT1 should be both enthalpically and entropically favored over the corresponding DM1r to DT1 conversion.

The *total* energies calculated by the current molecular mechanics approach have no intrinsic significance; only *relative* energies for identical systems calculated using the same method are meaningful. Thus, it is not possible to estimate the energy of the covalent complexes relative to the noncovalent complexes. The tetrahedral intermediates should, of course, be higher in energy than the initial noncovalent complex. The lower absolute energy calculated for the tetrahedral intermediates is due to the additional ionic interactions in the oxyanion hole present in these complexes that are absent in the noncovalent complexes.

We have modeled both the noncovalent Michaelis and covalent tetrahedral intermediate complexes for enzyme–substrate interaction with α-chymotrypsin using a significantly different approach from that of De Tar,[15] who considered only the tetrahedral intermediate, and Platzer et al.[14], who studied only the Michaelis complex. The approach presented here is an improvement over that of Platzer et al. where only very limited energy refinement was performed and that of De Tar, in which an artificial "buttressing potential" was used to clamp down the active-site cleft and only a few selected residues were allowed to energy refine. An important feature of our method is the use of computer graphics to rapidly generate different starting geometries for energy refinement. Although this does not solve the "local minimum problem", it allows one to consider a large number of possible structures very quickly, in order to search as much conformational space as possible. The use of computer graphics for the initial construction and evaluation of different geometries, followed by complete geometry optimization of the active site with *limited* restraints, to allow for minor conformational changes in the active-site structure in response to binding of different ligands, provides a consistent and physically reasonable approach for modeling noncovalent and covalent enzyme–substrate complexes.

We have not included the entire enzyme in these calculations, focusing instead on the residues within 7 Å of any atom of the substrate. It would have been possible, but prohibitively time consuming, to carry out calculations including the entire protein for each of the 18 structures considered in this study. However, our results suggest that the inclusion of the entire protein is not necessary for those proteins whose catalytic mechanisms do not involve large-scale conformational changes. We considered four different models of the active site, with varying degrees of motion allowed, ranging from a completely rigid active site to a completely flexible active site. The calculated stereoselectivity is strongly dependent on the ability of the active site to respond to ligand

(50) Knowles, J. R. *J. Theor. Biol.* **1965**, *9*, 213.
(51) Ingles, D. W.; Knowles, J. R. *Biochem. J.* **1968**, *108*, 561.

binding through conformational change; our results suggest that no stereoselectivity is possible with a rigid active site. It is encouraging that the most physically reasonable model, where only the α-carbons at the terminus of each peptide in the active-site model are restrained, produced results that gave the best overall agreement with experiment. Those portions of the enzyme that are missing from our model are primarily important in restraining motion at the end of each (artificial) peptide in our active site.

Our force field differs from those used by De Tar and Platzer et al.; we have essentially used the force field of Gelin and Karplus,[17] modified to include potentially hydrogen-bonding hydrogens explicitly. Our force field has not yet been extensively validated on small model systems, but the results obtained by the Karplus group[17] and ourselves[52] indicate that it contains no major defects.

We have not explicitly included solvent in these calculations, and this is clearly a drastic approximation. However, the general agreement with the experimental relative free energies of binding of the L and D enantiomers **1** and **2** suggests that differential solvation effects are not a key factor in α-chymotrypsin stereoselectivity. The relative energies of the tetrahedral intermediates are unlikely to be significantly modified by solvation of the complexes. In each tetrahedral intermediate, the O_1^- is in the oxyanion hole, the indole ring is buried in the hydrophobic pocket, the amino leaving group is in the solvent, and the carbonyl oxygen of the *N*-acetyl is oriented toward solvent. Thus, the solvent accessibilities of each group are similar for each complex so there should be little preferential solvation for one complex over another. For the more general case of modeling the energetics of the entire reaction pathway, a more realistic representation of solvent will be required.[21]

We have also neglected vibrational entropy effects. Hagler et al. have observed that the inclusion of such terms can change the relative energies of different polypeptide structural forms.[53] However, it is unlikely that the differences in these terms will be large enough for the enantiomers studied here to significantly effect our conclusions.

Summary

Molecular mechanics calculations on the Michaelis and tetrahedral intermediate enzyme–substrate complexes with α-chymotrypsin have demonstrated that such an approach can be useful in understanding the lack of stereoselectivity in the Michaelis complex and its presence in the tetrahedral intermediate. The substrate L-*N*-acetyltryptophanamide **1** and the inhibitor D-*N*-acetyltryptophanamide **2** are calculated to form noncovalent complexes with α-chymotrypsin that are similar in energy, where the D enantiomer is actually slightly more stable than the L. However, the tetrahedral intermediate for **1** is 9.3 kcal mol^{-1} lower in energy than the tetrahedral intermediate for **2**. The interactions involving the His-57 imidazolium hydrogen bond to the amino group of the substrate, the Ser-214-C=O···H *N*-acetylhydrogen bond, and the interaction of the indole ring with the hydrophobic pocket of the active site are the major features responsible for stereoselective differentiation of the L and D transition states (modeled by the tetrahedral intermediates). The His-57-N_{H_ϵ}···NH_2 interaction is critical not only because it provides much of the energetic basis for L–D stereoselectivity but because it puts the His-57 proton in excellent position to transfer to the amino leaving group of the substrate and form the acyl enzyme. In the D covalent complex, the His-57-N_{H_ϵ} is closer to to the O_γ of Ser-195 than to the amino group of the substrate, suggesting that the D tetrahedral intermediate is more likely to return to the initial Michaelis complex than to form the acyl enzyme. The calculated energies of the noncovalent and covalent complexes are consistent with the experimental observation that stereoselective recognition of L and D enantiomers must occur during the transition state rather than in the initial Michaelis complex.

Finally, it should be emphasized that correctly modeling the L–D stereoselectivity requires a flexible active site; with a rigid active site constrained to the initial X-ray coordinates, no stereoselectivity is possible. Our method, although obviously not the last word in theoretical calculations of enzyme–substrate interactions, provides one of the most practical and physically reasonable models of such complex systems at this time. Subsequent theoretical developments will be required to more generally elucidate enzyme specificity. In particular, development of a realistic approach to model the aqueous environment and its effect on the energies of bond making and breaking should allow a complete simulation of the reaction pathway, in addition to the estimation of relative energies at selected steps along the reaction pathway, which has been the focus of this study. However, it is likely that the developments reported and used in this study will also be useful in such subsequent studies.

Acknowledgment. P.A.K. is grateful to the NIH (CA-25644 and GM-29072) for support of this research. The calculations were carried out on the PDP-11/70 and the VAX-11/780 in the Computer Graphics Lab at UCSF, R. Langridge director, supported by the NIH (RR-1081). We are especially grateful to Professor A. Fink for his useful comments and his aid in modeling the best covalent L structure and to Professor P. Lehman for helpful discussions. G.W. has been supported by the NSF (U. S.–French Binational Fellowship) and by NATO (travel grant). J.M.B. was partially supported by the Americal Foundation for Pharmaceutical Education.

Note Added in Proof: We have subsequently improved the molecular mechanical model described in ref 45 and here (S. J. Weiner et al., to be submitted).

Registry No. 1, 2382-79-8; **2**, 7427-58-9; α-chymotrypsin, 9004-07-3.

Supplementary Material Available: Table IV and additional parameters for the tetrahedral intermediate (3 pages). Ordering information is given on any current masthead page.

(52) Dearing, A.; Weiner, P.; Kollman, P. *Nucleic Acids Res.* **1981**, *9*, 1483.

(53) Hagler, A. T.; Stern, P. S.; Sharon, R.; Becker, J. M.; Naider, F. *J. Am. Chem. Soc.* **1979**, *101*, 6842.